Synthesis, Crystal Structure and Characterization of a New Hydrogen-bonded Organic Framework①

SUN Jing[b] LIU Hai-Xiong[a②] LIU Tian-Fu[c②]

[a] (*Jinshan College, Fujian Agriculture and Forestry University, Fuzhou* 350002, *China*)

[b] (*School of Physical Science and Technology, ShanghaiTech University, Shanghai* 201210, *China*)

[c] (*State Key Laboratory of Structural Chemistry, Fujian Institute of Research on the Structure of Matter, Chinese Academy of Sciences, Fuzhou* 350002, *China*)

ABSTRACT The hydrogen-bonded organic framework (**PFC-32**), constructed by tetrahydroxyquinone (THQN) and diethylamine (DEA), was readily prepared via hydrothermal synthesis in DEF (N,N-diethylformamide). **PFC-32** was characterized by PXRD, IR, UV-Vis, TGA and photoluminescence (PL). Single crystal analysis reveals that **PFC-32** shows a three-dimensional (3D) framework, where the THQN anions are coplanar and separated by DEA cations. **PFC-32** displays intrinsic photoluminescence property owing to the alleviation of the aggregation-caused quenching (ACQ) effect caused by π-π stacking.

Keywords: tetrahydroyquinone, diethylamine, hydrogen-bonded organic framework;

DOI: 10.14102/j.cnki.0254–5861.2011–3113

1 INTRODUCTION

Porous architectures such as metal-organic frameworks (MOFs) and covalent organic frameworks (COFs), which possess distinctive pore structure and explicit reticular arrangement, have attracted significant attention in both crystal engineering and materials chemistry[1-5]. As a new branch of porous materials, hydrogen-bonded organic frameworks (HOFs) manifest unique superiority in structural design because of their low toxicity without any metal elements and promising potential as good candidates for bio-imaging, chemical sensing and drug delivery applications[6-9].

Constructing efficient fluorescence materials in the solid state has significant importance in materials science[10]. As established in solid state photochemistry, the fluorescence emission of aggregation phase is usually weaker than monomer due to the molecular π-π stacking in the condensed phase or the formation of excited complexes, which is known as aggregation-caused quenching (ACQ) effect[11-13]. This negative effect greatly restricts the applications of luminescent materials, such as bio-imaging and organic light emitting diodes (OLEDs). In recent years, researchers have been devoted to designing reasonable aggregated solid state aggregation luminescent molecule materials[14-16]. Compared to other condensed phase or excited complexes material, HOFs belong to porous framework materials with long-range order, with the monomers showing independent and orderly arrangement in space, and have great potential to be applied in the field of luminescent materials. However, the report on employing HOFs structures to eliminate or weaken ACQ effect is rare[17]. Herein, we report a novel three-dimensional (3D) hydrogen-bonding organic framework, namely **PFC-32**. Furthermore, we reveal the contribution and influence of crystal structure on the intrinsic fluorescence properties of the HOF material. This work may provide new insights into the design of effective solid state luminescent materials.

2 EXPERIMENTAL

2. 1 Materials and physical measurements

All chemicals were commercially purchased and used without any further purification. Single-crystal X-ray diffraction data were collected at 100 K on an Oxford Diffraction SuperNova diffractometer equipped with Cu-$K\alpha$

Received 22 January 2021; accepted 3 March 2021 (**CCDC 2061717**)

① Supported by Fujian Young and Middle-aged Teachers' Educational Research Project (No. JT180842)

② Corresponding authors. Liu Tian-Fu. E-mail: tfliu@fjirsm.ac.cn. Liu Hai-Xiong. E-mail: cgliuhx@126.com

radiation (λ = 1.5418 Å). The phase purity of the synthesized complex was examined by powder X-ray diffraction (PXRD). PXRD pattern was collected on a Rikagu Miniflex 600 Benchtop X-ray diffraction instrument. The solid-state fluorescence properties were measured at room temperature on an Edinburgh-instruments FS5 fluorescence spectrophotometer. Fourier transform infrared spectroscopy (FTIR) spectrum was obtained on a Bruker Spectrum in the range of 4000～250 cm^{-1} with KBr pellets. The UV-Vis absorption spectra were recorded on a PerkinElmer Lambda 950 spectrophotometer equipped with Labsphere intergrating in transmission mode at room temperature with $BaSO_4$ as a standard. Thermogravimetric analysis (TGA) was performed on a Seiko S-II instrument, and the dried crystalline samples were heated at a rate of 10 ℃/min up to 800 ℃ and then cooled to room temperature under N_2 atmosphere.

2. 2 Synthesis of PFC-32

A mixture of tetrahydroxyquinone (THQN) (30 mg, 0.175 mmol) and benzoic acid (15 mg, 0.123 mmol) was dissolved in DEF (1 mL) in a 10 mL Pyrex tube. Following that, 30 μL diethylamine (DEA) was added and sonicated for 5 min, and then sealed and put into a preheated oven at 120 ℃ for 48 h. The red block crystals of **PFC-32** suitable for single-crystal X-ray diffraction analysis were obtained. The crystals were collected by centrifugation and washed with acetone for several times until the supernatant solution became colorless.

2. 3 X-ray structure determination

Crystallographic data of the compound were collected on an Oxford Diffraction SuperNova diffractometer with Cu-*Kα* radiation (λ = 1.54184 Å) at 100 K under a cold nitrogen steam. The single crystal was coated with Paratone-N oil and mounted on a Nylon loop for diffraction. The collected frames were integrated using the preliminary cell-orientation matrix. CrysAlisPro software from Agilent Technologies was used for collecting the frames of data, indexing the reflections and determining the lattice constants. The structure was solved by direct methods and refined by full-matrix least-squares against F^2 through Olex 2 program package. All non-hydrogen atoms were refined with anisotropic displacement parameters, and the U_{iso}(H) were constrained to in general 1.2～1.5 times those of the parent atoms.

3 RESULTS AND DISCUSSION

3. 1 Structure determination

Single-crystal X-ray diffraction analysis revealed that **PFC-32** crystallizes in orthorhombic system, space group *Fmmm* with *a* = 8.6680(18), *b* = 11.7220(18), *c* = 16.976(3) Å, *V* = 1724.87 $Å^3$, *Z* = 4, the final *R* = 0.0494 and *wR* = 0.1364. The asymmetric unit contains one THQN anion and one DEA cation. Taken further analysis of the structure of **PFC-32**, each THQN anion interacts with four DEA cations through four N–H···O hydrogen bonds to extend into a three-dimensional (3D) layer. The N–H···O distances are 1.992 and 2.282 Å (Table 1). The structure can be more easily understood that THQN units are extended with each other, leading to a 2D layer along the *ab* plane, and then these layers are further interlinked by DEA cations to construct a 3D hydrogen-bonded organic framework. As shown in Fig. 1, all atoms of THQN ligands and N atoms of DEA ligands are absolutely coplanar, while C atoms of DEA locate at each side of the plane. The distance of THQN molecules in **PFC-32** is 5.861 Å separated by DEA molecules.

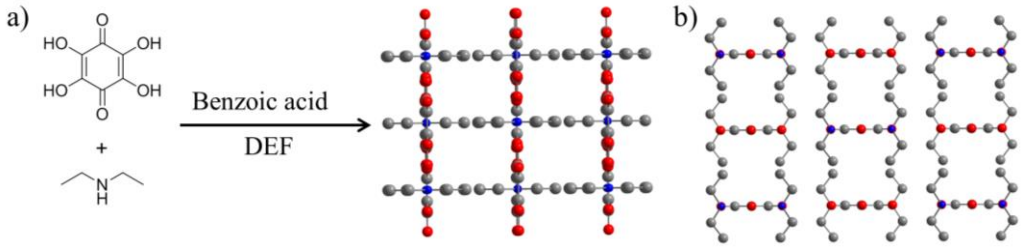

Fig. 1. a) Preparation and structure of PFC-32 (along the *c* axis). b) Structure of PFC-32 (along the *a* axis). For simplicity, hydrogen atoms are not shown

3. 2 PXRD analysis and IR spectra

Powder X-ray diffraction (PXRD) showed that the patterns of experimental **PFC-32** are in good agreement with the simulated patterns (Fig. 2a), confirming the phase purity of the synthesized complex. As shown in Fig. 2b, the peaks of THQN at 3390 and 3081 cm^{-1} are assigned to the free

O–H stretching and the hydrogen-bonded O–H groups, respectively[18]. Owing to the formation of hydrogen-bonding interactions, the peaks in **PFC-32** underwent a negative shift to 2982 and 2820 cm^{-1}, which are attributed to the hydrogen bonds between THQN and DEA. In addition, the downshift of C=O vibration from 1617 to 1518 cm^{-1} and the significant decrease at 1307 cm^{-1} correspond to the C–O stretching in **PFC-32**[19, 20], as a symbolic signal of the interaction of hydrogen bond. Meanwhile, the IR band at 2469 cm^{-1} was ascribed to the N–H stretching, as an evidence of the existence of DEA in **PFC-32**[21].

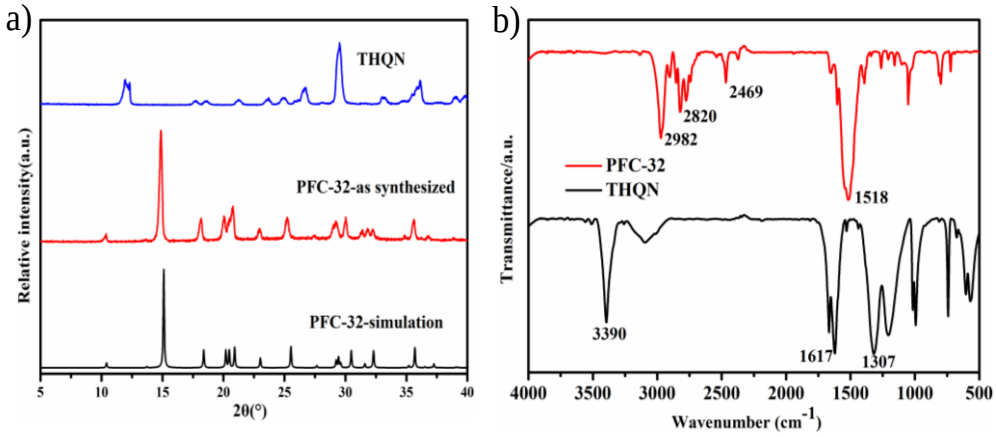

Fig. 2. a) PXRD characterization. b) FTIR spectra of PFC-32 compared to the pristine THQN

3. 3 UV-Vis spectra

Compared to pure THQN linkers (black in color), the (**PFC-32**) crystals are red as a result of the presence of DEA molecules. As shown in Fig. 3, the UV-Vis diffuse reflectance spectra (DRS) of **PFC-32** clearly exhibited a clear blueshift to 612 nm from 927 nm.

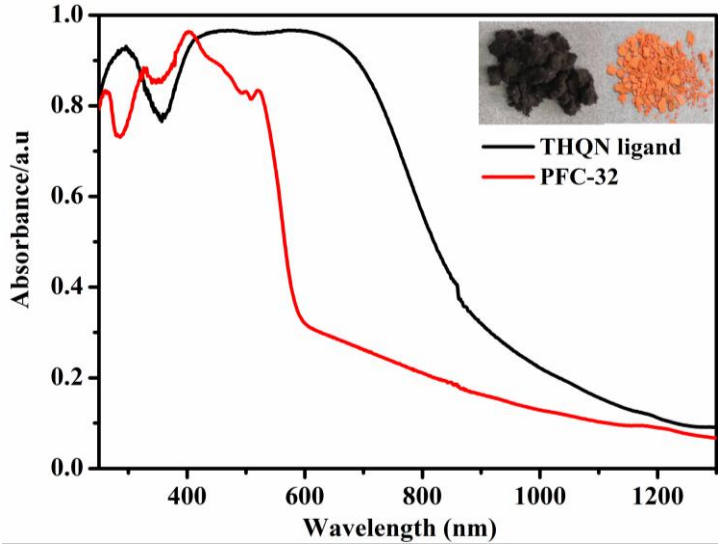

Fig. 3. UV-Vis diffuse reflectance spectra of PFC-32 compared to THQN ligand. Inset: the photographs of THQN ligand (left) and PFC-32 (right)

3. 4 Thermogravimetric analysis

Thermogravimetric analysis (TGA) of **PFC-32** is displayed in Fig. 4, which shows that the material can be stable to 200 ℃. The weight loss in the temperature ranges of 200～250 ℃ and 250～700 ℃ should correspond to the removal of DEA molecules (b.p = 55 ℃) and THQN ligand (b.p = 148 ℃), respectively. Thus, it reveals that **PFC-32** is much more thermal stable compared to DEA and THQN molecules, which may be attributed to the hydrogen bonds in **PFC-32**.

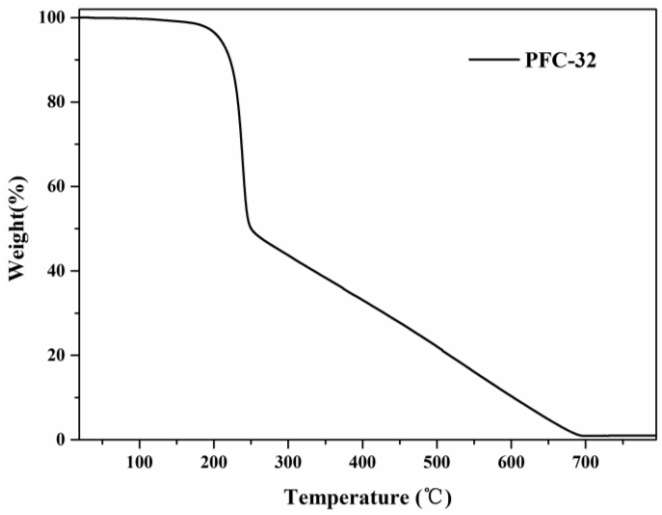

Fig. 4. TGA curve of PFC-32

3. 5 Fluorescence property

The fluorescence spectra of **PFC-32** crystals at room temperature are shown in Fig. 5a with a maximum at 595 nm (λ_{ex} = 480 nm). In contrast, the emission spectrum of THQN ligand indicated that it was almost fluorescence silent under the same excitation condition, which was caused by strong π-π stacking in condensed phase. As aforementioned in structure characteristics, THQN molecules in **PFC-32** were separated by DEA to reduce π-π stacking, corresponding to the distance of THQN molecules in **PFC-32** (5.861 Å). The presence of DEA and THQN synergistically enhanced fluorescence that cannot be achieved with either building blocks alone. To further confirm the mechanism of photoluminescence emission in **PFC-32**, the spectra of THQN ligand at different concentrations in DMF (Fig. 5b) showed the emission intensity decreased with the increase of THQN concentration. In high concentration of THQN, the molecules experienced stronger intermolecular interactions, which weakened the emission intensity.

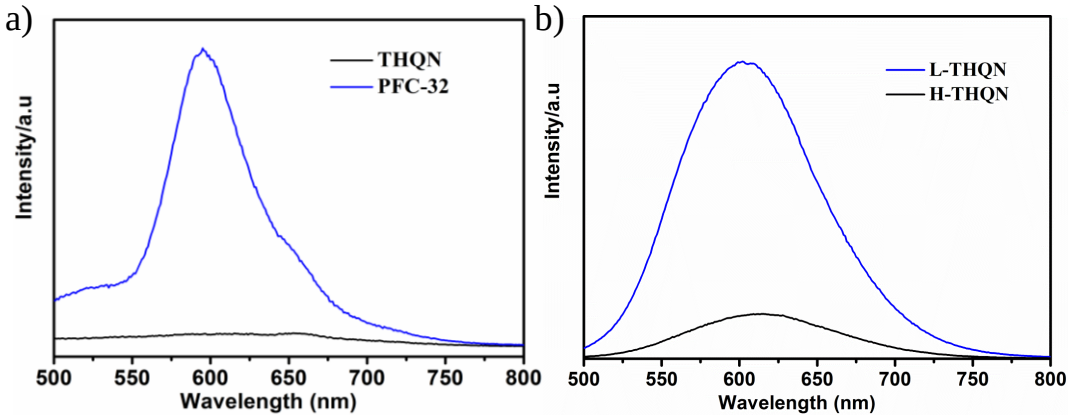

Fig. 5. a) PL emission spectra (excited at 480 nm) for PFC-32 and THQN. b) PL emission spectra (excited at 480 nm) for L-THQN and H-THQN. L-THQN was referred to low concentration of THQN (2 mg) in DMF (8 mL), while H-THQN was high concentration of THQN (2 mg) in DMF (4 mL)

Table 1. Hydrogen Bond Lengths (Å) and Bond Angles (°)

D–H···A	d(D–H)	d(H···A)	d(D···A)	∠DHA
N(1)–H(1B)···O(1)^{i}	0.92	2.28	9.475(14)	129
N(1)–H(1B)···O(2)^{ii}	0.92	1.99	8.419(19)	153

Symmetry transformation: i: –*x*+1, –*y*+1, *z*; ii: –*x*+1, –*y*+1, –*z*+1

Table 2. Selected Bond Lengths (Å) and Bond Angles (°)

Bond	Dist.	Bond	Dist.	Bond	Dist.
O(1)–C(1)	1.244(2)	C(2)–C(1)^{i}	1.476(2)	C(3)–C(4)	1.510(3)
O(2)–C(2)	1.245(3)	C(1)–C(1)^{ii}	1.478(2)		
C(2)–C(1)	1.476(2)	N(1)–C(3)^{iii}	1.485(2)		
Angle	(°)	Angle	(°)	Angle	(°)
O(2)–C(2)–C(1)^{i}	119.05(11)	O(1)–C(1)–C(2)	119.57(17)	C(3)–N(1)–C(3)^{iii}	114.68(19)
O(2)–C(2)–C(1)	119.05(11)	O(1)–C(1)–C(1)^{ii}	121.38(10)	N(1)–C(3)–C(4)	109.96(15)
C(1)–C(2)–C(1)^{i}	121.9(2)	C(2)–C(1)–C(1)^{ii}	119.05(11)		

Symmetry transformation: i: *x*, *y*, 1–*z*; ii: 2–*x*, 1– *y*, *z*; iii: 1–*x*, –*y*+1, *z*

Table 3. Crystal Data of the PFC-32

Empirical formula	$C_{14}H_{24}N_2O_6$	*Z*	4
CCDC number	2061717	ρ_{calc}/g/cm^3	1.218
Formula weight	316.35	μ/mm^{-1}	0.799
Temperature/K	100.0(2)	*F*(000)	680
Crystal system	Orthorhombic	Radiation	Cu-*Kα* (λ = 1.54178 Å)
Space group	*Fmmm*	2θ range for data collection/ °	5.1900 to 71.0640
a/Å	8.6680(18)	Index ranges	$-10 \leqslant h \leqslant 10$, $-14 \leqslant k \leqslant 10$, $-20 \leqslant l \leqslant 19$
b/Å	11.7220(18)	Reflections collected	950
c/Å	16.976(3)	Independent reflections	422 (R_{int} = 0.0163)
α/ °	90	Data/restraints/parameters	422/0/38
β/ °	90	Goodness-of-fit on F^2	1.075
γ/ °	90	Final *R* indexes ($I > 2\sigma(I)$)	R = 0.0492, wR = 0.1267
Volume/Å^3	1724.8(5)	Final *R* indexes (all data)	R = 0.0549, wR = 0.1364

4 CONCLUSION

In summary, a new hydrogen-bonded organic framework (**PFC-32**) was successfully constructed through hydrothermal synthesis. The ordered structure brings **PFC-32** intrinsic photoluminescence (PL) property owing to the alleviation of the aggregation-caused quenching (ACQ) effect caused by π-π stacking. Therefore, we demonstrated that this work provides new insights into the design of effective solid state luminescent materials.

REFERENCES

(1) Yin, Q.; Zhao, P.; Sa, R. J.; Chen, G. C.; Lu, J.; Liu, T. F.; Cao, R. An ultra-robust and crystalline redeemable hydrogen-bonded organic framework for synergistic chemo-photodynamic therapy. *Angew. Chem. Int. Ed. Engl.* **2018**, 57, 7691–7696.

(2) Cadiau, A.; Belmabkhout, Y.; Adil, K.; Bhatt, P. M.; Pillai, R. S.; Shkurenko, A.; Martineau-Corcos, C.; Maurin, G.; Eddaoudi, M. Hydrolytically stable fluorinated metal-organic frameworks for energy-efficient dehydration. *Science* **2017**, 356, 731–735.

(3) Shao, P.; Li, J.; Chen, F.; Ma, L.; Li, Q.; Zhang, M.; Zhou, J.; Yin, A.; Feng, X.; Wang, B. Flexible films of covalent organic frameworks with ultralow dielectric constants under high humidity. *Angew. Chem. Int. Ed. Engl.* **2018**, 57, 16501–16505.

(4) Huang, N.; Ding, X.; Kim, J.; Ihee, H.; Jiang, D. A photoresponsive smart covalent organic framework. *Angew. Chem. Int. Ed.* **2015**, 54, 8704–8707.

(5) Evans, A. M.; Parent, L. R.; Flanders, N. C.; Bisbey, R. P.; Vitaku, E.; Kirschner, M. S.; Schaller, R. D.; Chen, L. X.; Gianneschi, N. C.; Dichtel, W. R. Seeded growth of single-crystal two-dimensional covalent organic frameworks. *Science* **2018**, 7883.

(6) Cai, S.; Shi, H.; Zhang, Z.; Wang, X.; Ma, H.; Gan, N.; Wu, Q.; Cheng, Z.; Ling, K.; Gu, M.; Ma, C.; Gu, L.; An, Z.; Huang, W. Hydrogen-bonded organic aromatic frameworks for ultralong phosphorescence by intralayer π-π interactions. *Angew. Chem. Int. Ed. Engl.* **2018**, 57, 4005–4009.

(7) Li, Y. L.; Alexandrov, E. V.; Yin, Q.; Li, L.; Fang, Z. B.; Yuan, W.; Proserpio, D. M.; Liu, T. F. Record complexity in the polycatenation of three porous hydrogen-bonded organic frameworks with stepwise adsorption behaviors. *J. Am. Chem. Soc.* **2020**, 142, 7218–7224.

(8) Liu, B. T.; Pan, X. H.; Nie, D. Y.; Hu, X. J.; Liu, E. P.; Liu, T. F. Ionic hydrogen-bonded organic frameworks for ion-responsive antimicrobial membranes. *Adv. Mater.* **2020**, 32, e2005912.

(9) Li, Y. L.; Yin, Q.; Liu, T. F.; Cao, R.; Yuan, W. B. A novel porphyrin-based hydrogen-bonded organic framework. *Chin. J. Struct. Chem.* **2019**, 38, 2083–2088.

(10) Ye, Y. Z.; Lin, S.; Wu, X. J. Synthesis, structure and luminescent property of an europium(III) coordination polymer. *Chin. J. Struct. Chem.* **2014**, 33, 1649–1654.

(11) Yuan, W. Z.; Lu, P.; Chen, S.; Lam, J. W.; Wang, Z.; Liu, Y.; Kwok, H. S.; Ma, Y.; Tang, B. Z. Changing the behavior of chromophores from aggregation-caused quenching to aggregation-induced emission: development of highly efficient light emitters in the solid state. *Adv. Mater.* **2010**, 22, 2159–2163.

(12) Chen, Y.; Lam, J. W. Y.; Kwok, R. T. K.; Liu, B.; Tang, B. Z. Aggregation-induced emission: fundamental understanding and future developments. *Mater. Horiz.* **2019**, 6, 428–433.

(13) Lu, Z.; Wu, M.; Wu, S.; Yang, S.; Li, Y.; Liu, X.; Zheng, L.; Cao, Q.; Ding, Z. Modulating the optical properties of the AIE fluophor confined within UiO-66's nanochannels for chemical sensing. *Nanoscale* **2016**, 8, 17489–17495.

(14) Wang, H. P.; Wang, H. L.; Li, B. L. Synthesis, structure, luminescence and thermal stability properties of a new (3,4)-connected 2D Zn coordination polymer. *Chin. J. Struct. Chem.* **2020**, 39, 1835–1840.

(15) Li, J.; Wang, Y. H.; Song, R. F. A novel two-dimensional lead(II) coordination polymer based on dinuclear lead(II) unit containing (5-chloro-quinolin-8-yloxy) acetate. *Chin. J. Struct. Chem.* **2014**, 33, 1488–1494.

(16) Ding, S. P.; Zhang, Z. Y.; Zhou, G. J.; Cao, R. Synthesis, structure and luminescence properties of dumbbell-like silver clusters. *Chin. J Struct. Chem.* **2020**, 39, 1824–1834.

(17) Yu, T.; Ou, D.; Yang, Z.; Huang, Q.; Mao, Z.; Chen, J.; Zhang, Y.; Liu, S.; Xu, J.; Bryce, M. R.; Chi, Z. The HOF structures of nitrotetraphenylethene derivatives provide new insights into the nature of AIE and a way to design mechanoluminescent materials. *Chem. Sci.* **2017**, 8, 1163–1168.

(18) Wilsens, C. H. R. M.; Deshmukh, Y. S.; Noordover, B. A. J.; Rastogi, S. Influence of the 2,5-furandicarboxamide moiety on hydrogen bonding in aliphatic-aromatic poly(ester amide)s. *Macromolecules* **2014**, 47, 6196–6206.

(19) Jahan, M.; Bao, Q.; Loh, K. P. Electrocatalytically active graphene-porphyrin MOF composite for oxygen reduction reaction. *J. Am. Chem. Soc.* **2012**, 134, 6707–6713.

(20) Sk, M.; Grzywa, M.; Volkmer, D.; Biswas, S. Gas sorption and transition-metal cation separation with a thienothiophene based zirconium metal-organic framework. *J. Solid State Chem.* **2015**, 232, 221–227.

(21) Kumar, P.; Vahidzadeh, E.; Thakur, U. K.; Kar, P.; Alam, K. M.; Goswami, A.; Mahdi, N.; Cui, K.; Bernard, G. M.; Michaelis, V. K.; Shankar, K. C_3N_5: a low bandgap semiconductor containing an azo-linked carbon nitride framework for photocatalytic, photovoltaic and adsorbent applications. *J. Am. Chem. Soc.* **2019**, 141, 5415–5436.